J|A|C|S ARTICLES

Published on Web 10/28/2009

From 2-Fold Completive to Integrative Self-Sorting: A Five-Component Supramolecular Trapezoid

Kingsuk Mahata and Michael Schmittel*

Center of Micro- and Nanochemistry and Engineering, Organische Chemie I, Universität Siegen, Adolf-Reichwein-Strasse 2, D-57068 Siegen, Germany

Received August 25, 2009; E-mail: schmittel@chemie.uni-siegen.de

Abstract: The amalgamation of two *incomplete* self-sorting processes into a process that makes quantitative use of all members of the library is described by *2-fold completive* self-sorting. Toward this goal, individual metal−ligand binding scenarios were optimized for high thermodynamic stability and best selectivity, by screening a variety of factors, such as steric and electronic effects, $\pi-\pi$ interactions, and metal-ion specifics. Using optimized, heteroleptic metal−ligand binding motifs, a library of four different ligands (**1**, **2**, **3**, **4**) and two different metal ions (Zn^{2+}, Cu^{+}) was set up to assess 2-fold completive self-sorting. Out of 20 different combinations, the self-sorting library ended up with only two metal−ligand complexes in basically quantitative yield. To demonstrate the value of 2-fold completive self-sorting for the formation of nanostructures, the optimized, highly selective binding motifs were implemented into three polyfunctional ligands. Their integrative self-sorting in the presence of Zn^{2+} and Cu^{+} led to the clean formation of the supramolecular trapezoid **T**, a simple but still unknown supramolecular architecture. The dynamic trapezoid **T** consists of three different ligands with four different donor−acceptor interactions. Its structure was established by ^{1}H NMR spectroscopy, electrospray ionization mass spectroscopy, and differential pulse voltammetry (DPV) and by exclusion of alternative structures.

1. Introduction

The generation of complex, functional architectures from a diversity of different building blocks using noncovalent self-assembly along a self-sorting algorithm is quite common in nature. According to Darwin's "Survival of the Fittest" principle,[1] biological systems built on diversity and complexity can profit most from evolution and "Natural Selection" by the instatement of new emergent properties. Thus, the enhancement of complexity and multifariousness should be important for artificial supramolecular assemblies as well. Despite a notable wealth of self-assembled architectures published to date, the majority is comprised of a single unit (ligand) by using only one type of noncovalent interaction. As such, most of them lack diversity and will not be able to "excel" in our highly functional and sophisticated world.[2] Unsurprisingly, most of the known supramolecular architectures have been conceived to represent regular shapes, such as squares, rectangles, or other highly symmetric aggregates. To generate novel emergent properties, future artificial supramolecular species need to be composed of multiple components as well as multiple interactions.[2] Proper use of self-sorting would contribute to solve the problem.

A superb mastery of self-sorting is required[3] to concatenate different subunits with precise constitutional and/or positional control. Diverse self-sorting algorithms have to compete in multicomponent assemblies with their multitude of noncovalent interactions, with each product giving rise to a different free energy change. The thermodynamically controlled outcome, however, will depend upon the differences in Gibbs free energy ($\Delta\Delta G_{rxn}$) between all possible pathways. When $\Delta\Delta G_{rxn}$ is sufficiently large, a tangible difference in the products' population may be observed, with the process now being described as self-sorting. Seminal self-sorting systems based upon metal−ligand coordination,[4−9] hydrogen bonding,[10] solvophobic effects,[11] electrostatic interactions,[12] and dynamic covalent chemistry[13] have been developed during the past decade. However, the synthetic use of self-sorting is still in its infancy, and the enlargement of $\Delta\Delta G_{rxn}$ remains a challenge for chemists.

(1) Paul, D. B. *J. Hist. Biol.* **1988**, *21*, 411, and references cited therein.
(2) Schmittel, M.; Mahata, K. *Angew. Chem., Int. Ed.* **2008**, *47*, 5284.
(3) (a) Lehn, J.-M. *Science* **2002**, *295*, 2400. (b) Nitschke, J. R. *Acc. Chem. Res.* **2007**, *40*, 103. (c) Northrop, B. H.; Zheng, Y.-R.; Chi, K.-W.; Stang, P. J. *Acc. Chem. Res.* **2009**, *42*, 1554.
(4) Krämer, R.; Lehn, J.-M.; Marquis-Rigault, A. *Proc. Natl. Acad. Sci. U.S.A.* **1993**, *90*, 5394.
(5) Caulder, D. L.; Raymond, K. N. *Angew. Chem., Int. Ed.* **1997**, *36*, 1440.
(6) (a) Enemark, E. J.; Stack, T. D. P. *Angew. Chem., Int. Ed.* **1998**, *37*, 932. (b) Albrecht, M.; Schneider, M.; Röttele, H. *Angew. Chem., Int. Ed.* **1999**, *38*, 557. (c) Hwang, I.-W.; Kamada, T.; Ahn, T. K.; Ko, D. M.; Nakamura, T.; Tsuda, A.; Osuka, A.; Kim, D. *J. Am. Chem. Soc.* **2004**, *126*, 16187. (d) Schultz, D.; Nitschke, J. R. *Angew. Chem., Int. Ed.* **2006**, *45*, 2453. (e) Kamada, T.; Aratani, N.; Ikeda, T.; Shibata, N.; Higuchi, Y.; Wakamiya, A.; Yamaguchi, S.; Kim, K. S.; Yoon, Z. S.; Kim, D.; Osuka, A. *J. Am. Chem. Soc.* **2006**, *128*, 7670. (f) Saur, I.; Scopelliti, R.; Severin, K. *Chem.—Eur. J.* **2006**, *12*, 1058. (g) Barboiu, M.; Petit, E.; van der Lee, A.; Vaughan, G. *Inorg. Chem.* **2006**, *45*, 484. (h) Legrand, Y.- M.; van der Lee, A.; Barboiu, M. *Inorg. Chem.* **2007**, *46*, 9540. (i) Ghosh, S.; Turner, D. R.; Batten, S. R.; Mukherjee, P. S. *Dalton Trans.* **2007**, 1869. (j) Barboiu, M.; Dumitru, F.; Legrand, Y.-M.; Petit, E.; van der Lee, A. *Chem. Commun. (Cambridge)* **2009**, 2192.
(7) (a) Chi, K.-W.; Addicott, C.; Arif, A. M.; Stang, P. J. *J. Am. Chem. Soc.* **2004**, *126*, 16569. (b) Zhao, L.; Northrop, B. H.; Zheng, Y.-R.; Yang, H.-B.; Lee, H. J.; Lee, Y. M.; Park, J. Y.; Chi, K.-W.; Stang, P. J. *J. Org. Chem.* **2008**, *73*, 6580. (c) Rang, A.; Nieger, M.; Engeser, M.; Lützen, A.; Schalley, C. A. *Chem. Commun. (Combridge)* **2008**, 4789.

10.1021/ja907185k CCC: $40.75

In the area of supramolecular assemblies driven by self-sorting, Lehn et al.[4] described the spontaneous formation of helicates controlled by the number of binding sites in the ligands as well as by the preferred coordination geometry of the metal ions. Raymond et al.[5] reported on self-sorting of supramolecular triple helicates governed by the length of the ligands, whereas Stang et al. elaborated the simultaneous formation of different triangles, triangular prisms and squares, the latter being generated without formation of multiple diastereomers.[7,8] Very recently, Lehn et al. described an exhaustive study on controlling factors of self-sorting and reported about formation of metallomacrocycles.[9] In all cases self-sorting led either to the formation of multiple assemblies or formation of a single species along with free ligand. As such, the above processes were not making quantitative use of all members of the library, and such selection may be defined as *incomplete* self-sorting.

Chemists are interested in pure species, i.e., formation of a single nanoassembly,[14] and thus it is useful to exploit self-sorting in a manner that no members of the library are left over, generating a *completive* self-sorting library. A clever solution to this problem was reported by Schalley et al.,[12d] who used integrative[12c,15] self-sorting for the formation of a cascade-stoppered hetero[3]rotaxane. The same principle was applied later to fabricate multicomponent rectangles using three different components and two different interactions.[12e]

Among the various noncovalent binding tools to build intricate assemblies, metal coordination has turned out to be one of the most successful protocols. Thus, a wide range of self-assembled architectures has been established over the past 2 decades, utilizing metal−ligand coordination protocols.[16] We have contributed to this area by developing the HETPHEN[17] and HETTAP[18] concepts, both of which open an easy access to heteroleptic mononuclear complexes and equally to diverse supramolecular architectures.[18,19] In both concepts a quantitative self-sorting involving two donors and one acceptor (AD^1D^2 type) is involved, as the formation of the heteroleptic complex is favored over that of the two competing homoleptic complexes.[20]

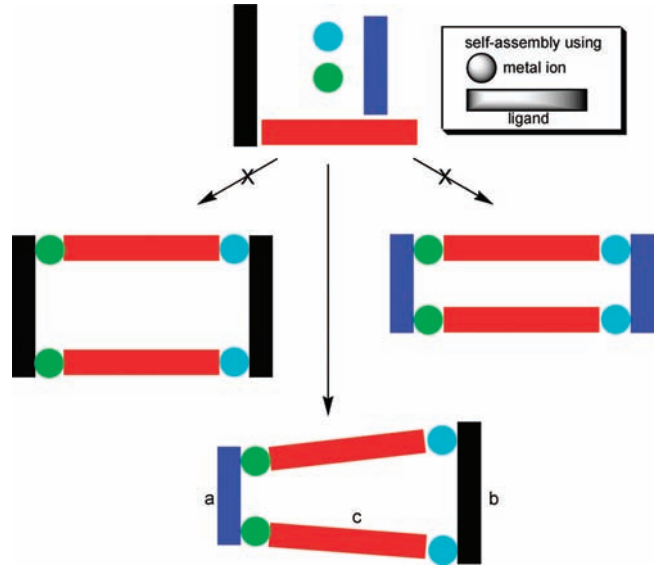

Figure 1. Self-sorting toward a five-component supramolecular isosceles trapezoid (cartoon).

It appeared to us that the HETPHEN and HETTAP concepts should open a venue to *2-fold completive* self-sorting, i.e., the event in which the combination of two incomplete self-sorting processes develop into a completive process by making quantitative use of all members of the library. Herein, we present the conceptual development of a library with four ligands and two metal ions that gives rise to the clean formation of two heteroleptic complexes out of 20 different possibilities; i.e., $A^1A^2D^1D^2D^3D^4 \rightarrow A^1D^1D^2 + A^2D^3D^4$. As a proof of concept and utility of 2-fold completive self-sorting, we fabricated a sophisticated nanoassembly, a dynamic five-component supramolecular isosceles trapezoid (Figure 1). We use here the definition of a trapezoid as a quadrilateral having *exactly* one pair of parallel sides, while the special case of an isosceles trapezoid requires additionally the other pair to be of equal length. Although the trapezoid is well present in nature, religion, and science, it is unknown, to the best of our knowledge, as an

(8) (a) Yang, H.-B.; Ghosh, K.; Northrop, B. H.; Stang, P. J. *Org. Lett.* **2007**, *9*, 1561. (b) Zheng, Y.-R.; Yang, H.-B.; Northrop, B. H.; Ghosh, K.; Stang, P. J. *Inorg. Chem.* **2008**, *47*, 4706. (c) Northrop, B. H.; Yang, H.-B.; Stang, P. J. *Inorg. Chem.* **2008**, *47*, 11257. (d) Zheng, Y.-R.; Yang, H.-B.; Ghosh, K.; Zhao, L.; Stang, P. J. *Chem.—Eur. J.* **2009**, *15*, 7203.

(9) Ulrich, S.; Lehn, J.-M. *J. Am. Chem. Soc.* **2009**, *131*, 5546.

(10) (a) Jolliffe, K. A.; Timmerman, P.; Reinhoudt, D. N. *Angew. Chem., Int. Ed.* **1999**, *38*, 933. (b) Xu, S.; Giuseppone, N. *J. Am. Chem. Soc.* **2008**, *130*, 1826. (c) Ghosh, S.; Wu, A.; Fettinger, J. C.; Zavalij, P. Y.; Isaacs, L. *J. Org. Chem.* **2008**, *73*, 5915. (d) Braekers, D.; Peters, C.; Bogdan, A.; Rudzevich, Y.; Böhmer, V.; Desreux, J. F. *J. Org. Chem.* **2008**, *73*, 701. (e) Ajami, D.; Hou, J.-L.; Dale, T. J.; Barrett, E.; Rebek, J, Jr. *Proc. Natl. Acad. Sci. U.S.A.* **2009**, *106*, 10430.

(11) (a) Bilgier, B.; Xing, X.; Kumar, K. *J. Am. Chem. Soc.* **2001**, *123*, 11815. (b) Schnarr, N. A.; Kennan, A. J. *J. Am. Chem. Soc.* **2003**, *125*, 667.

(12) (a) Liu, S.; Ruspic, C.; Mukhopadhyay, P.; Chakrabarti, S.; Zavalij, P. Y.; Isaacs, L. *J. Am. Chem. Soc.* **2005**, *127*, 15959. (b) Rekharsky, M. V.; Yamamura, H.; Ko, Y. H.; Selvapalam, N.; Kim, K.; Inoue, Y. *Chem. Commun. (Cambridge)* **2008**, 2236. (c) Wang, F.; Han, C.; He, C.; Zhou, Q.; Zhang, J.; Wang, C.; Li, N.; Huang, F. *J. Am. Chem. Soc.* **2008**, *130*, 11254. (d) Jiang, W.; Winkler, H. D. F.; Schalley, C. A. *J. Am. Chem. Soc.* **2008**, *130*, 13852. (e) Jiang, W.; Schalley, C. A. *Proc. Natl. Acad. Sci. U.S.A.* **2009**, *106*, 10425. (f) Rudzevich, Y.; Rudzevich, V.; Klautzsch, F.; Schalley, C. A.; Böhmer, V. *Angew. Chem., Int. Ed.* **2009**, *48*, 3867.

(13) Rowan, S. J.; Hamilton, D. G.; Brady, P. A.; Sanders, J. K. M. *J. Am. Chem. Soc.* **1997**, *119*, 2578.

(14) (a) Miyauchi, M.; Harada, A. *J. Am. Chem. Soc.* **2004**, *126*, 11418. (b) Rudzevich, Y.; Rudzevich, V.; Moon, C.; Schnell, I.; Fischer, K.; Böhmer, V. *J. Am. Chem. Soc.* **2005**, *127*, 14168.

(15) An *integrative* self-sorting system is characterized by the formation of one complex, in which more than two *different* subunits are bound in two or more recognition events with positional control; see ref 12d.

(16) (a) Leininger, S.; Olenyuk, B.; Stang, P. J. *Chem. Rev.* **2000**, *100*, 853. (b) Schmittel, M.; Kalsani, V. *Top. Curr. Chem.* **2005**, *245*, 1. (c) Severin, K. *Chem. Commun. (Cambridge)* **2006**, 3859. (d) Saalfrank, R. W.; Maid, H.; Scheurer, A. *Angew. Chem., Int. Ed.* **2008**, *47*, 8794. (e) Northrop, B. H.; Yang, H.-B.; Stang, P. J. *Chem. Commun. (Cambridge)* **2008**, 5896. (f) Zangrando, E.; Casanova, M.; Alessio, E. *Chem. Rev.* **2008**, *108*, 4979.

(17) (a) Schmittel, M.; Ganz, A. *Chem. Commun. (Cambridge)* **1997**, 999. (b) Schmittel, M.; Lüning, U.; Meder, M.; Ganz, A.; Michel, C.; Herderich, M. *Heterocycl. Commun.* **1997**, *3*, 493.

(18) (a) Schmittel, M.; Kalsani, V.; Kishore, R. S. K.; Cölfen, H.; Bats, J. W. *J. Am. Chem. Soc.* **2005**, *127*, 11544. (b) Schmittel, M.; He, B.; Mal, P. *Org. Lett.* **2008**, *10*, 2513. (c) Schmittel, M.; He, B. *Chem. Commun. (Cambridge)* **2008**, 4723. (d) Schmittel, M.; Mahata, K. *Inorg. Chem.* **2009**, *48*, 822.

(19) (a) Schmittel, M.; Ganz, A.; Fenske, D. *Org. Lett.* **2002**, *4*, 2289. (b) Schmittel, M.; Ammon, H.; Kalsani, V.; Wiegrefe, A.; Michel, C. *Chem. Commun. (Cambridge)* **2002**, 2566. (c) Schmittel, M.; Kalsani, V.; Fenske, D.; Wiegrefe, A. *Chem. Commun. (Cambridge)* **2004**, 490. (d) Schmittel, M.; Kishore, R. S. K. *Org. Lett.* **2004**, *6*, 1923. (e) Kishore, R. S. K.; Paulat, T.; Schmittel, M. *Chem.—Eur. J.* **2006**, *12*, 8136. (f) Schmittel, M.; Kalsani, V.; Michel, C.; Mal, P.; Ammon, H.; Jäckel, F.; Rabe, J. P. *Chem.—Eur. J.* **2007**, *13*, 6223.

(20) D = donor, A = acceptor; out of three possibilities (AD^1D^1, AD^1D^2, AD^2D^2) only one complex (AD^1D^2) formation was observed due to self-sorting.

Chart 1. Ligands Used for Self-Sorting

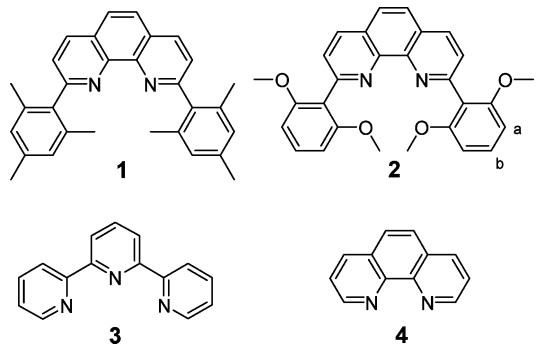

Scheme 1. Self-Sorting Leading to Heteroleptic Complex Formation

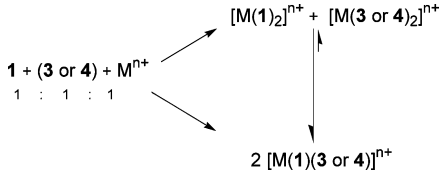

artificial supramolecular assembly and can be considered as of higher order than other literature-known quadrilaterals, such as the square, rectangle, etc.[21]

2. Results and Discussion

2.1. Self-Sorting in a $AD^1D^2D^3$ Library: Using the Zn^{2+} Ion. To stimulate self-sorting among multiple ($n \geq 2$) donor−acceptor pairs, we have evaluated and refined the HETPHEN and HETTAP approaches.[17,18] Both concepts are based on the use of **1**, a bulky 2,9-diaryl-substituted phenanthroline (Chart 1), whose front-side shielding prevents the formation of the homoleptic $[M(\mathbf{1})_2]^{n+}$ with $M^{n+} = Cu^+$, Ag^+, Zn^{2+}. However, in combination with a sterically unassuming counterpart (e.g., **3** or **4**) ligand **1** will furnish quantitatively the heteroleptic metal complex $[M(\mathbf{1})(\mathbf{3}\text{ or }\mathbf{4})]^{n+}$, given the correct stoichiometry. Similarly, for **2** the homoleptic complex $[Cu(\mathbf{2})_2]^+$ is precluded in MeCN, whereas $[Zn(\mathbf{2})_2]^{2+}$ is possible.[18a] Hence, for copper(I) the heteroleptic complexes $[Cu(\mathbf{2})(\mathbf{3}\text{ or }\mathbf{4})]^+$ are accessible. All heteroleptic complexes $[M(\mathbf{1}\text{ or }\mathbf{2})(\mathbf{3}\text{ or }\mathbf{4})]^{n+}$ profit from the extra thermodynamic stability arising by the $\pi-\pi$ interaction of the aryl groups of **1**,**2** and ligand **3**,**4**, rendering them more stable than the homoleptic complexes $[M(\mathbf{3}\text{ or }\mathbf{4})_2]^{n+}$ (Scheme 1).[17,18]

How can we arrange for 2-fold completive self-sorting in a putative $A^1A^2D^1D^2D^3D^4$ library composed of four ligands **1**−**4** as donors and two metal ion M^{n+} as acceptors? On the basis of the HETPHEN and HETTAP concepts, we can only exclude the formation of the homoleptic complexes $[M(\mathbf{1})_2]^{n+}$ and $[M(\mathbf{2})_2]^{n+}$ as well as of the heteroleptic complex $[M(\mathbf{1})(\mathbf{2})]^{n+}$. All other combinations should show up more or less. Thus, to differentiate the energetic stability of all possible heteroleptic complexes involving the shielded ligands **1** and **2**, we needed to instill some beneficiary factor already on the level of a smaller $AD^1D^2D^3$ library. As our previous study with two shielded ligands did not show the required selectivity,[18a] we turned our attention to ligand **2**, which has four methoxy groups for additional coordination with a suitable metal ion. Indeed, it is known[9] that O-donor atoms may provide extra coordination when the metal ion needs donating substituents in the coordination shell.

Scheme 2. $AD^1D^2D^3$ Type Self-Sorting Using Zn^{2+} Ion

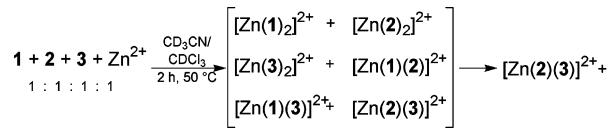

To investigate initially $AD^1D^2D^3$ self-sorting, a dynamic library was generated from the three different ligands **1**−**3** in the presence of Zn^{2+} (Scheme 2) to evaluate the controlling factors (sterics, maximum site occupancy, and $\pi-\pi$ stacking). Ligands **1**−**3** and Zn^{2+} were taken up in equimolar amounts (1:1:1:1) in $CD_3CN/CDCl_3$ (3:1) and were sonicated at 50 °C for 2 h. The resultant yellow solution was characterized by ^1H NMR and electrospray ionization mass spectroscopy. Three different ligands in the presence of a metal ion may form six different complexes (Scheme 2). However, the number is reduced as a combination of analytical ^1H NMR and mass data clearly suggested. Electrospray ionization mass spectra (ESI-MS) of the library evidenced the presence of $[Zn(\mathbf{2})(\mathbf{3})]^{2+}$ along with free ligand **1** (Figure 2). A singly charged species at $m/z = 897.8$ and a doubly charged species at $m/z = 374.6$ were observed after the loss of one and two OTf^- counteranions, respectively. Characteristic peaks of the other heteroleptic complex, i.e., of $[Zn(\mathbf{1})(\mathbf{3})]^{2+}$, were hardly visible.[22] ^1H NMR of the library also unambiguously supported the self-sorting behavior (Figure 3). Diagnostic signals of the heteroleptic complex $[Zn(\mathbf{2})(\mathbf{3})]^{2+}$ showed up at 6.01 and 6.87 ppm, corresponding to the aromatic substituents of **2** (doublet for a-H at 6.01 ppm and triplet for b-H at 6.87 ppm; Chart 1). A sharp singlet for the mesityl ArH protons of **1** at 6.17 ppm would have been characteristic of the heteroleptic complex $[Zn(\mathbf{1})(\mathbf{3})]^{2+}$, but no such signal was detectable in that region. Rather, a singlet at 6.95 ppm, diagnostic of the uncomplexed ligand **1**, was observed. Thus, a combination of both analytical data suggested self-sorting behavior.

The self-sorting may be rationalized as follows: Formation of $[Zn(\mathbf{1})_2]^{2+}$ is impossible due to steric reasons as outlined above, while, in contrast, both other homoleptic complexes $[Zn(\mathbf{2})_2]^{2+}$ and $[Zn(\mathbf{3})_2]^{2+}$ are feasible as well as all the heteroleptic combinations. Our previous study,[18a] however, suggests that in such case the output always favors heteroleptic combination. The 1:1:1:1 stoichiometry along with maximum site occupancy and full consumption of the zinc salt incites either the formation of a heteroleptic complex along with a free ligand or a mixture of heteroleptic complexes with some amount of the two shielded ligands left unused. The heteroleptic combination $[Zn(\mathbf{1})(\mathbf{2})]^{2+}$ is less likely due to high steric crowding at the metal ion. The most probable outcomes are, thus, $[Zn(\mathbf{1})(\mathbf{3})]^{2+}$ or $[Zn(\mathbf{2})(\mathbf{3})]^{2+}$. The higher thermodynamic stability of the $[Zn(\mathbf{2})(\mathbf{3})]^{2+}$ may arise from the additional coordination of one methoxy group to yield a hexacoordinated zinc ion and/or the higher σ basicity of the methoxy groups substituted ligand **2**. In contrast, the other heteroleptic complex $[Zn(\mathbf{1})(\mathbf{3})]^{2+}$ can only realize pentacoordination of the zinc center.

To get further insight into the role of the metal−ligand interaction, we turned our attention to Cu^+ complexes, since

(21) For the construction of squares or rectangles only one or two ligands are necessary, whereas for the trapezoid at least three ligands are required.

(22) For comparison we prepared pure $[Zn(\mathbf{1})(\mathbf{3})]^{2+}$ and $[Zn(\mathbf{2})(\mathbf{3})]^{2+}$: ^1H NMR spectra of the complexes are shown in Figure 3.

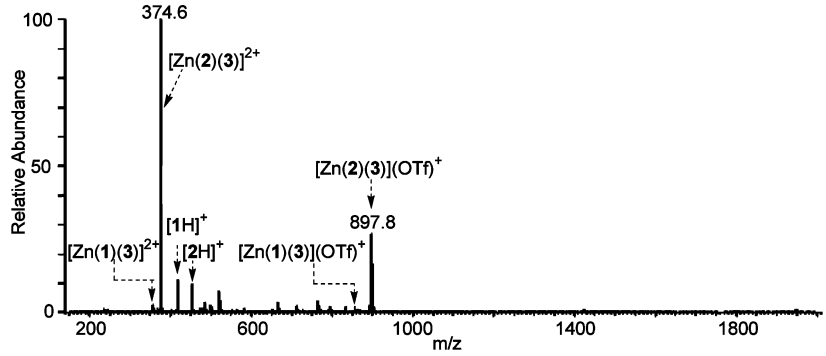

Figure 2. ESI-MS of an equimolar mixture of **1**−**3** in the presence of Zn^{2+} in a mixture of MeCN/$CHCl_3$ (3:1).

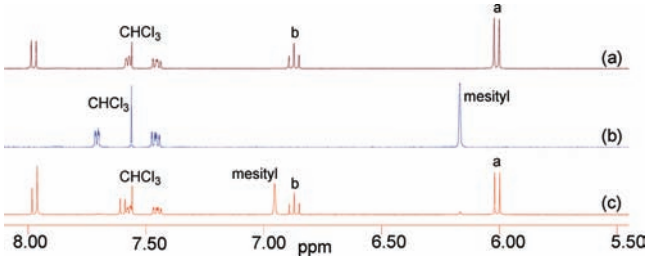

Figure 3. Partial ^1H NMR (400 MHz, 298 K) spectra of (a) [Zn(**2**)(**3**)]$(OTf)_2$, (b) [Zn(**1**)(**3**)]$(OTf)_2$, and (c) self-sorting library among **1**−**3** in the presence of Zn^{2+} in CD_3CN/CD_3Cl (3:1).

Scheme 3. $AD^1D^2D^3$ Type Self-Sorting Using Cu^+ Ion

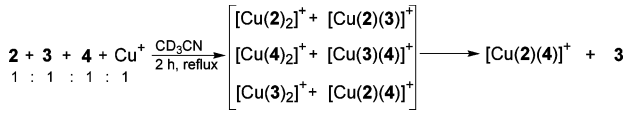

their tetrahedral coordination environment is limited to four metal−donor interactions, even if the surrounding ligands provide more than four donor atoms.[23] As a consequence, we studied the reaction of an equimolar mixture of **1**, **2**, and **4** (Chart 1) in the presence of Cu^+. In the clear red solution, formation of both heteroleptic complexes [Cu(**1**)(**4**)]$^+$ and [Cu(**2**)(**4**)]$^+$ was observed in almost similar quantity, as evidenced from ^1H NMR and ESI-MS (Supporting Information). The finding that the heteroleptic complex containing the methoxy-substituted ligand **2** is not dominating precludes its higher σ basicity to be a decisive factor. Applying this insight to the self-sorting with zinc suggests that the dominating [Zn(**2**)(**3**)]$^{2+}$ is profiting mostly from a direct coordination of one methoxy group driving the sorting process and that such scenario is specific to Zn^{2+} due to its tendency to build octahedral complexes.

2.2. Self-Sorting in a $AD^1D^2D^3$ Library: Using Cu^+ Ion. To set up a complementary sorting process to the above complexation scenario of two shielded ligands along with one unshielded ligand, we decided to interrogate the competition of two unshielded ligands with a shielded ligand (Scheme 3). The library was generated by mixing ligands **2**−**4** along with Cu^+ in a 1:1:1:1 molar ratio at ambient atmosphere. After refluxing the mixture in acetonitrile for 2 h, the red solution was characterized by ^1H NMR, ESI-MS, and differential pulse voltammetry (DPV). All analytical methods attested to the exclusive formation of [Cu(**2**)(**4**)]$^+$ along with free **3**. In particular, the ESI-MS of the mixture showed only a peak corresponding to [Cu(**2**)(**4**)]$^+$ at 695.1 (Figure 4). No peak was observed that would correspond to other complexes.

Another proof of evidence arises from diagnostic ^1H NMR signals of the aromatic substituents of **2** (doublet for a-H and triplet for b-H). In the independently prepared complex [Cu(**2**)(**4**)]$^+$ they appear at 5.72 (for a-H) and at 6.41 ppm (for b-H), whereas those protons appear at 6.09 and at 6.89 ppm in [Cu(**2**)(**3**)]$^+$. In the library mixture only signals appear at 5.72 ppm and at 6.41 ppm, as shown in Figure 5, allowing to conclude that only [Cu(**2**)(**4**)]$^+$ is present.

Further proof of self-sorting was observed from DPV through a comparison of the oxidation potentials of [Cu(**2**)(**4**)]$^+$ and [Cu(**2**)(**3**)]$^+$. In the pure complex [Cu(**2**)(**4**)]$^+$ the copper(I) oxidation occurs at 0.29 V_{SCE}, whereas in [Cu(**2**)(**3**)]$^+$ it appears at −0.21 V_{SCE}. A single peak at 0.29 V_{SCE} after self-sorting furthermore demonstrated exclusive formation of [Cu(**2**)(**4**)]$^+$ (Supporting Information).

Among the six different possibilities, $\pi-\pi$ stacking is possible in all complexes involving **2**. However, as the homoleptic complex [Cu(**2**)$_2$]$^+$ cannot form in acetonitrile,[16b] the most favorable combinations are either [Cu(**2**)(**3**)]$^+$ or [Cu(**2**)(**4**)]$^+$. In Cu^+ complexes, the metal ion is generally tetrahedrally

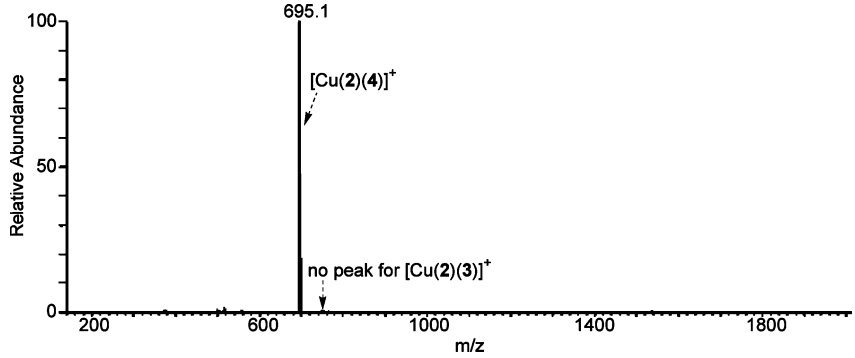

Figure 4. ESI-MS of an equimolar mixture of **2**−**4** in the presence of Cu^+ in a mixture of MeCN/$CHCl_3$ (3:1).

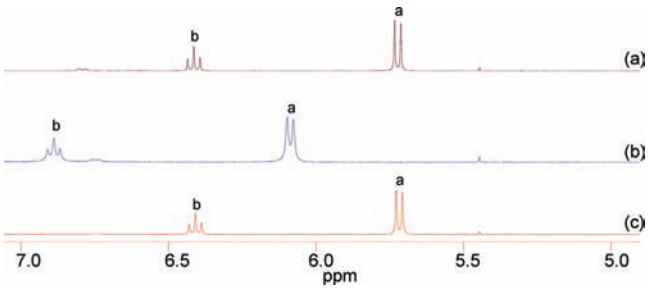

Figure 5. Partial ^{1}H NMR (400 MHz, 298 K) spectra of (a) [Cu(**2**)(**4**)](PF$_6$), (b) [Cu(**2**)(**3**)](PF$_6$), and (c) self-sorting library with **2**, **3**, and **4** in the presence of Cu$^+$ in CD$_3$CN.

coordinated by four donor atoms, even if the surrounding ligands provide more than four of those.[23] Accordingly, in [Cu(**2**)(**3**)]$^+$ the terpyridine ligand **3** ought to behave as a bischelate 2,2′-bipyridine, leaving one pyridine unit unused. As the 2,2′-bipyridine is a weaker binding ligand than **4**, [Cu(**2**)(**4**)]$^+$ is expected to be the most stable complex.

2.3. A^{1}A^{2}D^{1}D^{2}D^{3}D^4 Self-Sorting. Combining the insight from both experiments above, we designed a 2-fold completive library from **1**−**4** and Zn^{2+}/Cu$^+$, with the goal that self-sorting would make full use of all constituents leading exclusively to [Cu(**1**)(**4**)]$^+$ and [Zn(**2**)(**3**)]$^{2+}$. One has to note that self-sorting in AD^{1}D^{2}D^3 libraries had been effectively providing [Zn(**2**)(**3**)]$^{2+}$, but it was not successful with [Cu(**1**)(**4**)]$^+$ as the latter was formed in an even amount together with [Cu(**2**)(**4**)]$^+$. The expectation for A^{1}A^{2}D^{1}D^{2}D^{3}D^4 self-sorting was, however, that—given the right stoichiometry—the full depletion of ligands **2** and **3** through formation of [Zn(**2**)(**3**)]$^{2+}$ would drive the formation of [Cu(**1**)(**4**)]$^+$. These considerations suggested use of an equimolar mixture of **1**−**4** (1:1:1:1) with the same amount of Zn^{2+} and Cu$^+$ (1:1). After refluxing this reaction mixture in acetonitrile for 2 h, the resultant solution was characterized by ^{1}H NMR, ESI-MS, and DPV. Theoretically, 20 different complexes, all enumerated in Scheme 4, may form. Rewardingly, ESI-MS of the reaction mixture furnished evidence of a highly successful self-sorting, furnishing basically only two products. In line with such a statement, the ESI-MS showed only two major species, a doubly charged one at $m/z = 374.7$ corresponding to [Zn(**2**)(**3**)]$^{2+}$ and a single one at $m/z = 659.2$ corresponding to [Cu(**1**)(**4**)]$^+$ (Figure 6).

In the diagnostic region of the ^{1}H NMR spectrum only one set of signals was observed for each shielded phenanthroline **1** and **2**, suggesting their involvement in only one type of complex. A triplet at 6.87 ppm along with a doublet at 6.02 ppm (characteristic of [Zn(**2**)(**3**)]$^{2+}$) and a singlet at 5.95 ppm (characteristic of [Cu(**1**)(**4**)]$^+$) clearly demonstrated the dominant presence of the heteroleptic species [Zn(**2**)(**3**)]$^{2+}$ and [Cu(**1**)(**4**)]$^+$ in solution (Supporting Information), in full agreement with the ESI-MS data.

Further unambiguous confirmation of the self-sorting process was accomplished through the electroanalytical study of the copper(I) complexes by DPV. In DPV, the independently prepared complexes [Cu(**1**)(**4**)]$^+$ and [Cu(**2**)(**4**)]$^+$ exhibited well-separated oxidation waves with $E_{1/2} = 0.44$ V$_{SCE}$ and $E_{1/2} = 0.29$ V$_{SCE}$, respectively, that remained distinguishable after mixing (Figure 7). A single oxidation peak at $E_{1/2} = 0.44$ V$_{SCE}$ from the library mixture thus confirmed the presence of only one copper(I) complex, supporting the formation of [Cu(**1**)(**4**)]$^+$.

The exclusive formation of the heteroleptic complexes [Zn(**2**)(**3**)]$^{2+}$ and [Cu(**1**)(**4**)]$^+$ in the above self-sorting highlights one more time the extra stabilization gained from $\pi-\pi$ stacking, sterics, and maximum site occupancy. As noticed earlier in section 2.2, the parent phenanthroline **4** prefers to combine with the tetracoordinate Cu$^+$ ion (Scheme 3), leaving two choices: the heteroleptic copper(I) complexes [Cu(**1**)(**4**)]$^+$ and [Cu(**2**)(**4**)]$^+$. On the other hand, Zn^{2+} favors a higher coordination number than four and thus will combine preferentially with **3** in a heteroleptic zinc(II) complex. The most probable zinc(II) complexes are thus [Zn(**1**)(**3**)]$^{2+}$ and [Zn(**2**)(**3**)]$^{2+}$. In light of the stoichiometric situation chosen, a combination of either [Cu(**1**)(**4**)]$^+$ and [Zn(**2**)(**3**)]$^{2+}$ or [Cu(**2**)(**4**)]$^+$ and [Zn(**1**)(**3**)]$^{2+}$ is expected. According to the results in section 2.2, [Cu(**1**)(**4**)]$^+$ and [Cu(**2**)(**4**)]$^+$ have comparable stabilities. However, [Zn(**2**)(**3**)]$^{2+}$ is thermodynamically more stable than [Zn(**1**)(**3**)]$^{2+}$, biasing the global system toward [Cu(**1**)(**4**)]$^+$ and [Zn(**2**)(**3**)]$^{2+}$ as the favored combination.

2.4. Supramolecular Trapezoid. Design Criteria. To demonstrate the value of our 2-fold completive self-sorting protocol for nanostructure fabrication, we decided to exploit the selection observed in section 2.3 for the fabrication of a five-component supramolecular isosceles trapezoid. A look at the required binding situation in an isosceles trapezoid (Figure 1) suggested to control the required linkage of the unequal sides *a* and *b* to *c* by utilizing the preferential formation of [Cu(**2**)(**4**)]$^+$ and [Zn(**1**)(**3**)]$^{2+}$ (Scheme 4). As a result, the coordination properties of **1** and **2** were implemented into the bisphenanthrolines **5**[24] and **6** (=sides *a* and *b*), whose lengths (Chart 2) were varied in a way to allow the unstrained construction of the trapezoid. Likewise, the binding motifs of **3** and **4** were instigated into the phenanthroline−terpyridine hybrid **7**, which represents side *c* in our approach.

Synthesis of the new ligand **6** was carried out along a general procedure described by our group.[24] After introducing the aromatic groups at positions 2 and 9 of the phenanthroline **8**, two phenanthroline subunits **11** were connected by means of a Sonogashira cross-coupling[25] reaction as described in Scheme 5. For the synthesis of **7**, 3-ethynylphenanthroline (**12**) was reacted with the terpyridine unit **13** under solvent-free Sonogashira conditions.[25]

Despite the use of two selective heteroleptic coordination motifs, implemented into **5**−**7**, formation of trapezoid **T** is not

Scheme 4. A^{1}A^{2}D^{1}D^{2}D^{3}D^4 Type Self-Sorting Using Two Metal Ions and Four Ligands

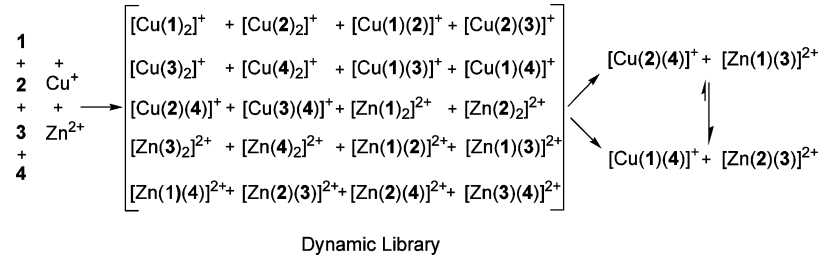

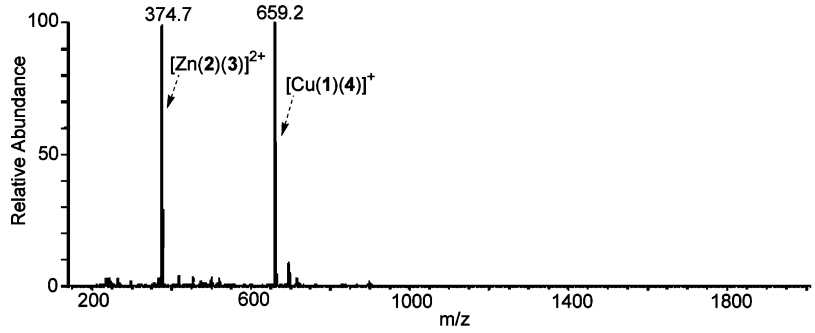

Figure 6. ESI-MS of an equimolar mixture of **1**−**4** in the presence of Zn^{2+} and Cu^{+} in MeCN.

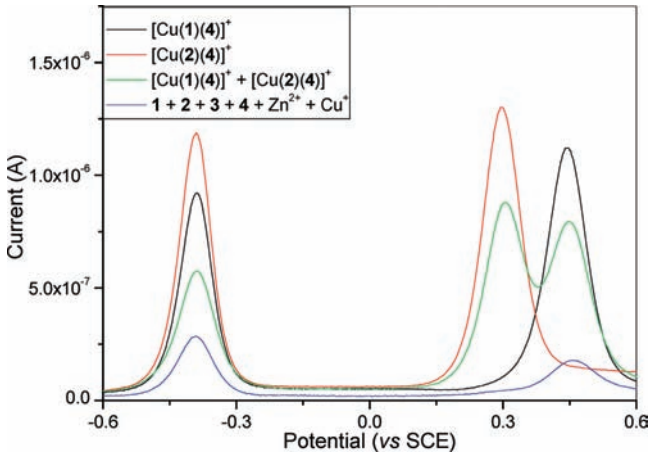

Figure 7. Differential pulse voltammograms of $[Cu(\mathbf{1})(\mathbf{4})]^{+}$ (black), $[Cu(\mathbf{2})(\mathbf{4})]^{+}$ (red), a mixture of $[Cu(\mathbf{2})(\mathbf{4})]^{+}$ and $[Cu(\mathbf{1})(\mathbf{4})]^{+}$ (green), and the self-sorting library (blue). All measurements were done in acetonitrile with 0.1 M nBu$_4$NPF$_6$ as electrolyte against a Ag wire as a quasi-reference electrode and 2,4,6-triphenylpyrylium tetrafluoroborate as internal standard (scan rate of 20 mV s^{-1} and a pulse height of 2 mV).

necessarily warranted (Scheme 6). Theoretically, three ligands in the presence of two different types of metal ions may lead to several self-assembled structures. However, considering the stability of the different complexes as a result of the chosen heteroleptic coordination motifs (see sections 2.1−2.3), one may expect the formation of three architectures, as depicted in Scheme 6: a trapezoid **T**, a small rectangle $\mathbf{R_S}$ (=$[Cu_2Zn_2(\mathbf{5})_2(\mathbf{7})_2]^{6+}$), and a large rectangle $\mathbf{R_L}$ (= $[Cu_2Zn_2(\mathbf{6})_2(\mathbf{7})_2]^{6+}$). If we predict the relative stability of each architecture, then $\mathbf{R_S}$ is expected to be the least stable entity due to the fact that it contains the motif $[Zn(\mathbf{1})(\mathbf{3})](OTf)_2$ being less stable than $[Zn(\mathbf{2})(\mathbf{3})](OTf)_2$.

Preparation of the Trapezoid. The self-sorting of small building units in sections 2.1 and 2.2 was effected by mixing components together and by reacting them for 2 h to achieve self-correction. For the construction of the trapezoid **T**, though, we decided to reduce mismatch and high kinetic barriers for self-correction by applying a sequential addition protocol. Thus, a mixture of **6** and **7** was first treated with Zn^{2+} (1:2:2 ratio) in CD_3CN. After sonication at 60 °C for 2 h, ligand **5** and Cu^{+} (1:2 ratio) were added, and the resulting mixture was further sonicated at the same temperature for 8 h. The clear orange-red solution was characterized by ESI-MS, ^{1}H NMR, and DPV.

ESI-MS spectra showed dominantly peaks corresponding to $\mathbf{T}$ = $[Cu_2Zn_2(\mathbf{5})(\mathbf{6})(\mathbf{7})_2](OTf)_4(PF_6)_2$; as in the spectral region of m/z = 150−2000 a series of intense peaks (at m/z = 614.4, 766.5, 995.6 and 1376.9) corresponding to the trapezoid was detected (Figure 8). The most abundant peaks showed up at m/z = 614.4 and at m/z = 766.5 that correspond to **T** after the loss of six and five counteranions, respectively, i.e., $[Cu_2Zn_2(\mathbf{5})(\mathbf{6})(\mathbf{7})_2]^{6+}$ and $[Cu_2Zn_2(\mathbf{5})(\mathbf{6})(\mathbf{7})_2(OTf)]^{5+}$. Except the signals characteristic for the trapezoid, some fragmentations were also observed in negligible percentage. The five-charged peak at m/z = 519.0 should be associated with $[CuZn_2(\mathbf{6})(\mathbf{7})_2(MeCN)]^{5+}$, the doubly charged one at m/z = 637.5 with $[Cu_2(\mathbf{5})(MeCN)_2]^{2+}$, the triply charged peak at m/z = 660.2 with $[CuZn(\mathbf{6})(\mathbf{7})]^{3+}$, and the doubly charged one at m/z = 957.4 with $[Zn(\mathbf{6})(\mathbf{7})]^{2+}$. Most importantly, we did not observe any signals corresponding to the large rectangle $\mathbf{R_L}$ = $[Cu_2Zn_2(\mathbf{6})_2(\mathbf{7})_2]^{6+}$ or the small rectangle $\mathbf{R_S}$ = $[Cu_2Zn_2(\mathbf{5})_2(\mathbf{7})_2]^{6+}$. The absence of characteristic signals for $\mathbf{R_S}$ (m/z = 568.8, 712.5, 926.8, and 1285.2; Supporting Information) allowed us to conclude that the formation of the trapezoid is basically quantitative.

The exclusive formation of the trapezoid **T** was further evidenced from the ^{1}H NMR spectrum, in particular analyzing the signals of bisphenanthroline **6** as it contains several protons (b-H, b′-H, c-H, and methoxy protons) with peaks in a diagnostic

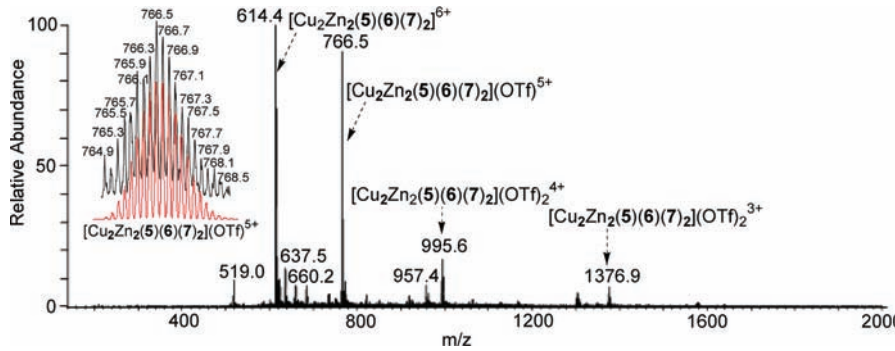

Figure 8. ESI-MS spectrum of a solution of trapezoid **T** in acetonitrile along with isotopic distributions (black, experimental; red, calculated) for $[Cu_2Zn_2(\mathbf{5})(\mathbf{6})(\mathbf{7})_2](OTf)^{5+}$.

Chart 2. Ligands Used for Synthesis of the Supramolecular Trapezoid **T**

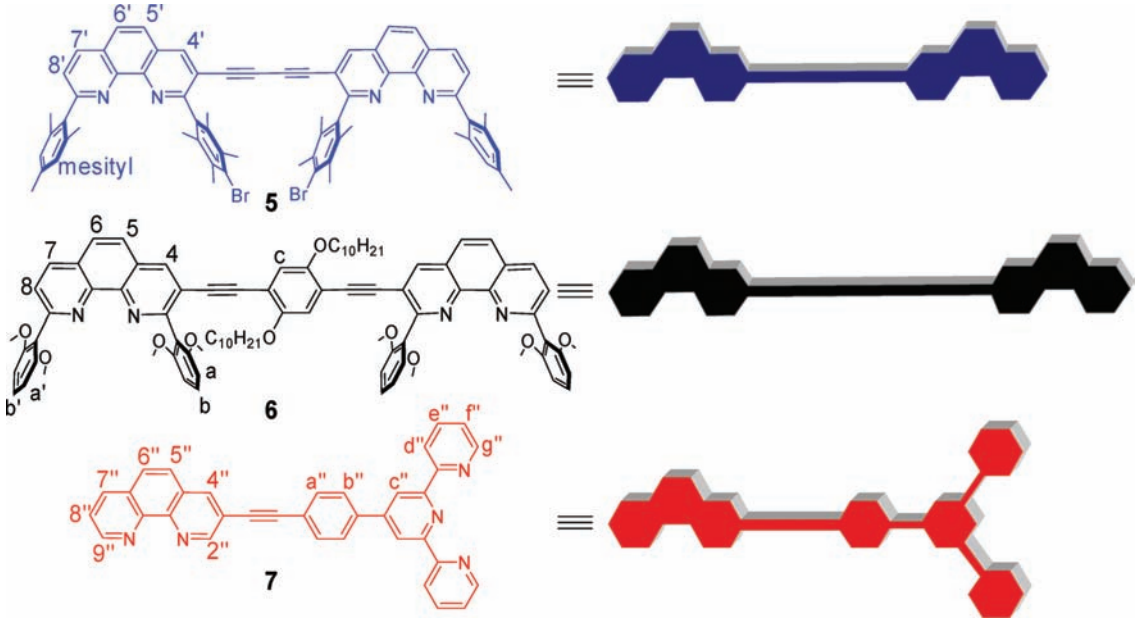

Scheme 5. Synthesis of Ligands **6** and **7**

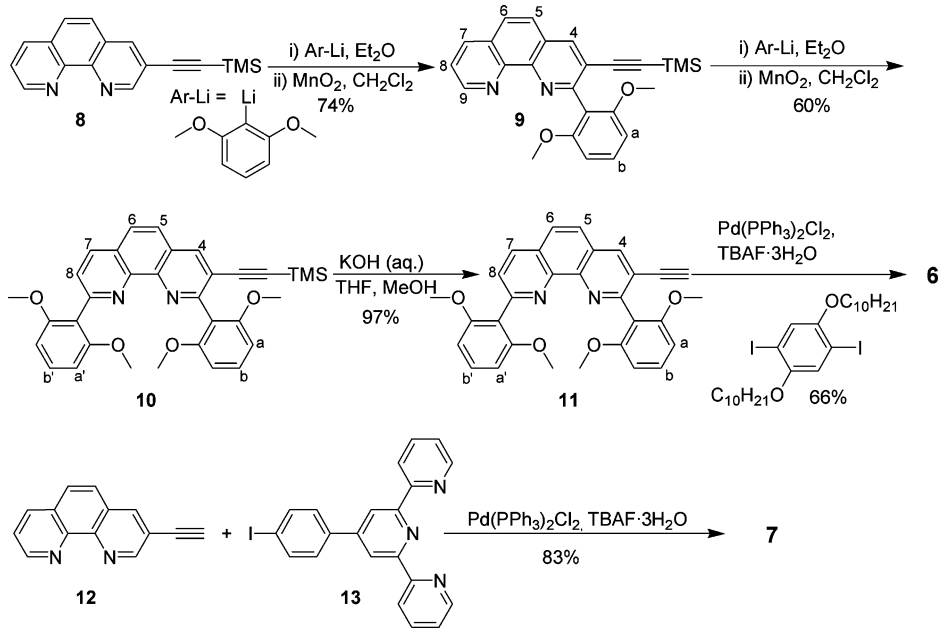

region. Due to the stereogenic axis formed at the HETPHEN binding centers, two diastereomers are possible in **T** (similar to $\mathbf{R_L}^{\mathbf{A}}$ and $\mathbf{R_L}^{\mathbf{B}}$), as indicated by the ^{1}H NMR spectra (Figure 9c). Two singlets at 6.37 and at 6.40 ppm (c-H) supported the presence of two diastereomeric trapezoids **T** in a ca. 1:1 ratio. To further corroborate the constitutional connectivity of the ligands at the metal centers of **T**, we synthesized the rack assembly $[Zn_2(\mathbf{6})(\mathbf{3})_2](OTf)_4$ (Scheme 7) as it mimics the [Zn(terpy of **7**)(**6**)]$^{2+}$ centers of **T** closely. The rack was afforded from a mixture of **6**,**3**, and Zn^{2+} in CD_3CN at 60 °C for 2 h using the appropriate stoichiometry. A comparison between the ^{1}H NMR spectra of the trapezoid and the rack showed that diagnostic signals (methoxy-, b-, and b′-H of ligand **6**) appeared in identical regions of both spectra: in the spectrum of rack $[Zn_2(\mathbf{6})(\mathbf{3})_2](OTf)_4$ (Figure 9a) these protons appeared at 2.76−2.81 ppm (methoxy protons) and at 6.83−6.89 ppm (b-, b′-H), whereas in **T** they showed up at 2.71−2.85 ppm (methoxy protons) and at 6.71−6.89 ppm (b-, b′-H). This agreement confirms that in **T** the terpyridine moiety of **7** is exclusively linked via a zinc metal center with **6**. There is, however, a difference between **T** and the rack. In **T**, due to the existence of two diastereomers, the methoxy groups are diastereotopic and hence eight singlets are expected. Due to overlap in the ^{1}H NMR, only five singlets were observed, though. Similarly, three out of four triplets for b-protons and b′-protons were observed.

For further corroboration of the structure of **T**, we prepared the rectangle $\mathbf{R_L}$ from a mixture of **6** and **7** with Cu^+ and Zn^{2+}

(23) Medlycott, E. A.; Hanan, G. S. *Chem. Commun. (Cambridge)* **2007**, 4884.
(24) Schmittel, M.; Michel, C.; Wiegrefe, A.; Kalsani, V. *Synthesis* **2001**, 1561.
(25) Liang, Y.; Xie, Y.-X.; Li, J.-H. *J. Org. Chem.* **2006**, *71*, 379.

Scheme 6. Synthesis of Self-Sorted Supramolecular Trapezoid **T**

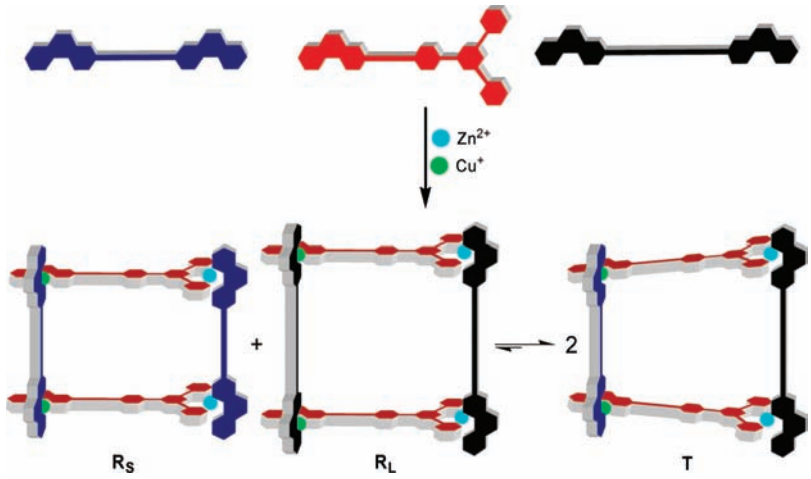

Scheme 7. Synthesis of Rack Assembly $[Zn_2(\mathbf{6})(\mathbf{3})_2](OTf)_4$

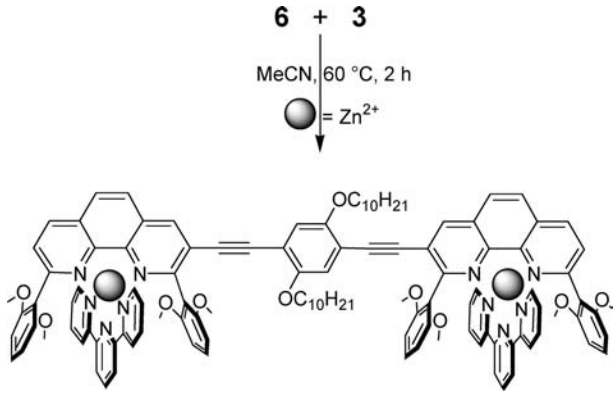

(1:1:1:1) in acetonitrile at 60 °C for 12 h. The ESI-MS of the assembly was quite clean, exhibiting only peaks corresponding to $\mathbf{R_L}$ (Supporting Information). In contrast, the ^{1}H NMR was complicated (Figure 9b) due to the presence of several isomers (two pairs of constitutionally different diastereomers; Figure 10). In rectangle $\mathbf{R_L}$, two different types of metal ions can coordinate to the same bisphenanthroline (as in the case of $\mathbf{R_L}^{\mathbf{A}}$ and $\mathbf{R_L}^{\mathbf{B}}$) or to different bisphenanthrolines (as in the case of $\mathbf{R_L}^{\mathbf{C}}$ and $\mathbf{R_L}^{\mathbf{D}}$). Such a complicated scenario is not possible in **T** as Cu^+ will preferentially coordinate to **5** and Zn^{2+} to **6**.

An evaluation of the methoxy peaks of **6** clearly establishes the absence of any large rectangles $\mathbf{R_L}$ in the self-sorting mixture containing **T** (Figure 9b,c). Accordingly, in the ^{1}H NMR of $\mathbf{R_L}$ the methoxy protons of **6** appear in two regions: for $[M(terpy)(\mathbf{6})]^{n+}$ centers they appear at 2.68−2.82 ppm, whereas for $[M(phen)(\mathbf{6})]^{n+}$ centers they show up at 3.19−3.39 ppm. In the self-sorting mixture containing **T** no signals are present in the region of 3.19−3.39 ppm. Unfortunately, the small rectangle $\mathbf{R_S}$ did not provide diagnostic ^{1}H NMR signals for comparison. However, since **T** is clearly not contaminated with $\mathbf{R_L}$, which should be accompanied by $\mathbf{R_S}$ in the same stoichiometric amount, the presence of $\mathbf{R_S}$ can be excluded as well.

We also studied the redox behavior of **T**. It is well-known in the literature that despite a similar electronic environment the redox potential may vary with geometry (e.g., angles between ligands).[18b] As **T** exists in two diastereomeric forms with its different geometric settings, two dissimilar potentials may be expected. Experimentally, for **T** a broad peak was observed (Figure 11), but deconvolution allowed the determination of two individual redox potentials at 0.61 and 0.67 V_{SCE} that may be assigned to the two diastereomers. Both values are quite distinct from $E_{1/2} = 0.44$ V_{SCE} found for $[Cu(\mathbf{1})(\mathbf{4})](PF_6)$. However, such differences are not unusual and possibly due to the electronic discrepancy of the ligands as well as the different geometric scenarios. For a similar HETPHEN complex, a constraint

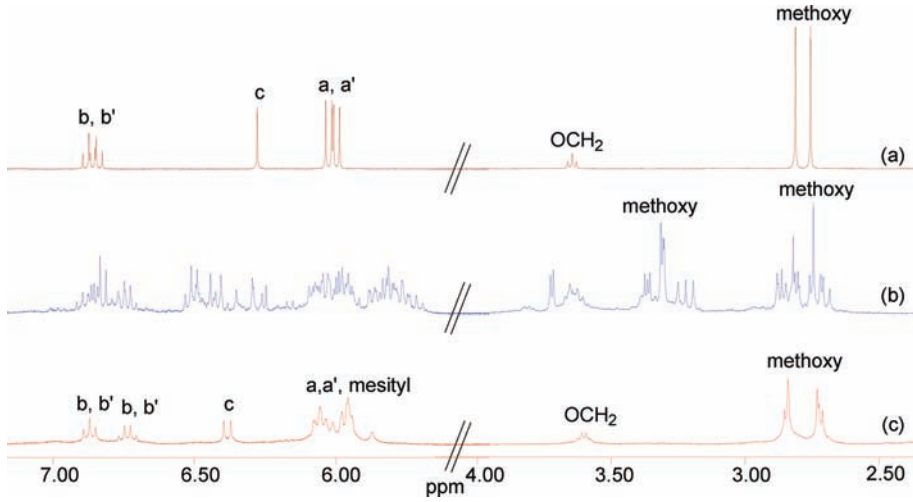

Figure 9. Partial ^{1}H NMR (400 MHz, 298 K) spectra of (a) rack $[Zn_2(\mathbf{6})(\mathbf{3})_2](OTf)_4$, (b) large rectangle $\mathbf{R_L}$, and (c) trapezoid **T** in CD_3CN. Due to the existence of four diastereomers of $\mathbf{R_L}$, the ^{1}H NMR is complicated.

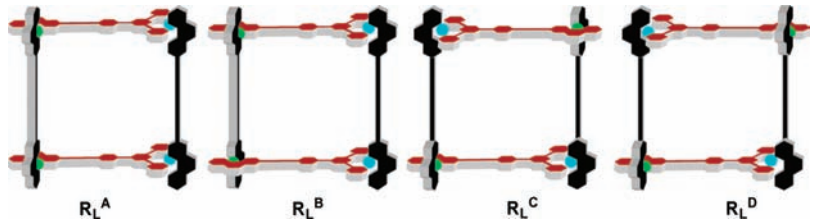

Figure 10. Four isomers of the large rectangle $\mathbf{R_L}$ (two pairs of constitutionally different diastereomers).

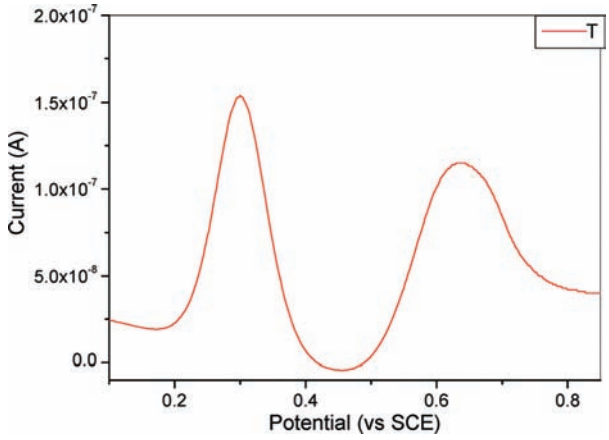

Figure 11. Differential pulse voltammgram of trapezoid **T** in acetonitrile with 0.1 M nBu$_4$NPF$_6$ as electrolyte against a Ag wire as a quasi-reference electrode and dimethylferrocene as internal standard (scan rate of 20 mV s^{-1} and a pulse height of 2 mV).

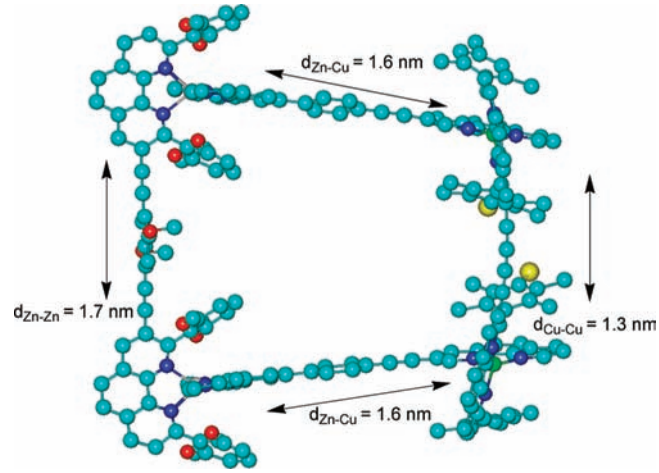

Figure 12. Energy-minimized structure of the supramolecular trapezoid **T** (hydrogen atoms are removed for clarity). Counter anions are not included.

triangle, the oxidation potential was reported even higher ($E_{1/2}$ = 0.83 V_{SCE}).[26] From the deconvolution we also determined the individual population of each diastereomers ((51 ± 1):(49 ± 1)). Both ^{1}H NMR integration and deconvoluted DPV spectra thus suggest formation of both diastereomers in equal amounts (Supporting Information).

To get some insight into the geometry of the trapezoid, we performed force field computations (MM+ as implemented into Hyperchem 7.52) and molecular dynamics simulations. For the computations, the long alkyl chains of ligand **6** were replaced by methyl groups and no symmetry constraints were set. The energy minimized structure of **T** is depicted in Figure 12. It exhibits a $Zn^{2+}-Zn^{2+}$ distance of 1.68 nm and a $Cu^{+}-Cu^{+}$ distance of 1.25 nm. The short $Zn^{2+}-Cu^{+}$ distances amount to 1.60 and 1.62 nm, whereas the diagonal $Zn^{2+}-Cu^{+}$ distances are 2.18 and 2.14 nm.

In summary, we have been able to prepare a trapezoid in solution from the self-assembly of ligands **5**−**7** in the presence of the metal ions, copper(I) and zinc(II). Considering the relative stability of the architectures **T**, $\mathbf{R_S}$, and $\mathbf{R_L}$, $\mathbf{R_S}$ is expected to be the least stable entity due to the fact that it contains the motif [Zn(**1**)(**3**)](OTf)$_2$ being less stable than [Zn(**2**)(**3**)](OTf)$_2$. On the other hand, **T** and $\mathbf{R_L}$ have the same situation about the Zn^{2+} complex and a similar set up at the Cu^{+} complexation site. Due to the difference in length of **5** and **6** in **T** the geometry at the metal coordination centers is not perfect. Thus, along a reasonable stability sequence the large rectangle $\mathbf{R_L}$ is expected to be the most stable entity: $\mathbf{R_L} > \mathbf{T} > \mathbf{R_S}$. For the global reaction outcome, however, not the individual energy of a species, but the total energy of the ensemble is of importance. As we started off with the same amount of **5** and **6**, the formation of rectangle $\mathbf{R_L}$ will be paralleled by an equal amount of $\mathbf{R_S}$.

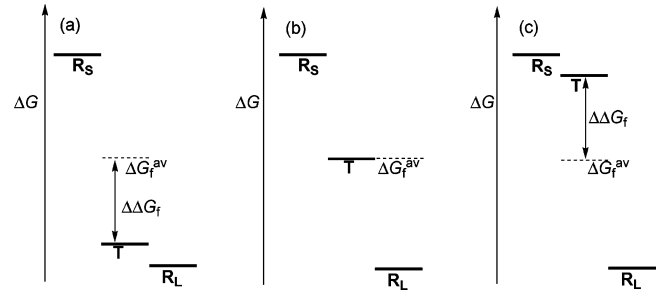

Figure 13. Relative energy of the rectangles $\mathbf{R_L}$ and $\mathbf{R_S}$ and of the trapezoid **T**.

On the basis of the Gibbs free energy of formation of the trapezoid ΔG_f (**T**) and the averaged free energy of formation ΔG_f^{av} of the two rectangles, $\Delta G_f^{av} = [\Delta G_f (\mathbf{R_S}) + \Delta G_f (\mathbf{R_L})]/2$), three different scenarios, as depicted in a qualitative manner in Figure 13, are possible. If ΔG_f^{av} of the two rectangles is comparable with the Gibbs free energy of formation ΔG_f (**T**) of the trapezoid, i.e., $2\Delta\Delta G_f \sim 0$, then all three architectures will form in parallel (Figure 13b).

In the case of $\Delta G_f^{av} > \Delta G_f(\mathbf{T})$ (Figure 13a), the system will prefer to exist in trapezoid form. In such a case, one molecule of $\mathbf{R_S}$ and one molecule of $\mathbf{R_L}$ will dynamically reassemble into two molecules of **T** and the system will gain an overall energy of $2\Delta\Delta G_f$. On the contrary, there will be an equimolar mixture of two rectangles without occurrence of **T** if $\Delta G_f^{av} < \Delta G_f(\mathbf{T})$ (Figure 13c).

Level of Complexity. At this point it may be instructive to evaluate the level of complexity reached with the preparation of **T**, because, clearly, not all self-sorting systems are of the same quality. As a quantifiable criterion for the level of complexity, the degree of self-sorting (M) may be defined as

(26) Schmittel, M.; Mahata, K. *Chem. Commun. (Cambridge)* **2008**, 2550.

$M = P/P_0$ with P representing the number of possibilities and P_0 representing the number of produced complexes in the mixture. For the clean generation of a mononuclear HETPHEN or HETTAP complex, a situation typical for a AD^1D^2 type self-sorting, $P = 3$ and thus M becomes 3. Self-sorting described in sections 2.1 and 2.2 is of the $AD^1D^2D^3$ type. Here $M = 6$, as only one product is formed out of six possibilities. For the self-sorting described in section 2.3 involving a $A^1A^2D^1D^2D^3D^4$ type setting providing two products, $M = 10$. Unfortunately, in the case of the trapezoid the determination of the level of complexity along the above formula becomes impracticable as there is an infinite number of oligomeric aggregates possible.

3. Conclusions

In conclusion, we have utilized steric effects, $\pi-\pi$ interactions, electronic effects, and metal−ion interactions to control integrative self-sorting toward the formation of the trapezoid **T**. To the best of our knowledge, **T** is the first supramolecular trapezoid, a dynamic entity that contains three different bifunctional ligands and two different metal ions. Such structural diversity in a small aggregate may be applied to combine molecular subunits, even leading to emergent molecular machines.[27] Furthermore, such diversity may be translated into 3D architectures, as 3D architectures are often combinations of 2D architectures. For example, a cube is a collection of several squares.

To develop a self-sorting strategy for **T**, the individual coordination units of the three bifunctional ligands had to be optimized. Along with a search to improve formation of mononuclear heteroleptic complexes in mixtures of ligands and metal ions, we have investigated increasingly more complex libraries starting from AD^1D^2 type self-sorting ($M = 3$), to $AD^1D^2D^3$ self-sorting ($M = 6$) toward 2-fold completive self-sorting described in a $A^1A^2D^1D^2D^3D^4$ library ($M = 10$).

4. Experimental Section

4.1. General Methods. All commercial reagents were used without further purification. The solvents were dried with appropriate desiccants and distilled prior to use. Silica gel 60 (70−230 mesh) was used for column chromatography. ^{1}H NMR and ^{13}C NMR were recorded on a Bruker Avance 400 MHz spectrometer using the deuterated solvent as the lock and residual solvent as the internal reference. NMR measurements were carried out at 298 K. The following abbreviations were utilized to describe peak patterns: s = singlet, d = doublet, t = triplet, and m = multiplet. The numbering of the carbon atoms of the molecular formulas shown in the Experimental Section is only used for the assignments of the NMR signal and is not in accordance with the IUPAC nomenclature rules. Electrospray ionization mass spectra were recorded on a Thermo-Quest LCQ Deca. Differential pulse voltammetry was measured on a Parstat 2273 in dry acetonitrile. Melting points were measured on a Büchi SMP-20 and are uncorrected. Infrared spectra were recorded using a Varian 1000 FT-IR instrument. Elemental analysis measurements were done using an EA 3000 CHNS. Precursors for **6**[24] and **7**[28] were synthesized according to known procedures. The energy minimized structure was computed with the MM^+ force field as implemented in Hyperchem 7.52.

4.2. Characterization and Preparation of Compounds. Synthesis of the new ligand **6** was carried out along a general procedure described by our group.[24]

2-(2,6-Dimethoxyphenyl)-3-(trimethylsilanylethynyl)[1,10]-phenanthroline (9). Yield 74%; mp 211 °C; ^{1}H NMR (400 MHz, $CDCl_3$) δ 0.04 (s, 9 H, $SiMe_3$), 3.68 (s, 6 H, OMe), 6.63 (d, ^3J = 8.4 Hz, 2 H, a-H), 7.32 (t, ^3J = 8.4 Hz, 1 H, b-H), 7.57 (dd, ^3J = 8.0 Hz, ^3J = 4.4 Hz, 1 H, 8-H), 7.74 (d, ^3J = 8.8 Hz, 1 H, 6-H), 7.77 (d, ^3J = 8.8 Hz, 1 H, 5-H), 8.20 (dd, ^3J = 8.0 Hz, ^4J = 1.8 Hz, 1 H, 7-H), 8.35 (s, 1 H, 4-H), 9.19 (dd, ^3J = 4.4 Hz, ^4J = 1.8 Hz, 1 H, 9-H); ^{13}C NMR (100 MHz, $CDCl_3$) δ −0.3, 55.9, 99.6, 102.5, 104.0, 119.0, 120.9, 122.8, 126.1, 126.7, 126.8, 129.1, 129.6, 135.8, 138.4, 145.0, 146.3, 150.5, 158.3, 158.5; IR (KBr) ν 3420, 3000, 2956, 2899, 2835, 2360, 2149, 1616, 1599, 1588, 1549, 1489, 1474, 1453, 1433, 1411, 1401, 1306, 1290, 1250, 1223, 1175, 1111, 1057, 1035, 1027, 997, 906, 860, 842, 829, 822, 787, 763, 736, 691, 639; ESI-MS m/z (%) 413.2 (100) $[M + H]^+$. Anal. Calcd for $C_{25}H_{24}N_2O_2Si$: C, 72.78; H, 5.86; N, 6.79. Found: C, 72.49; H, 5.80; N, 6.74.

2,9-Bis(2,6-dimethoxyphenyl)-3-(trimethylsilanylethynyl)[1,10]-phenanthroline (10). Yield 60%; mp > 260 °C; ^{1}H NMR (400 MHz, $CDCl_3$) δ 0.05 (s, 9 H, $SiMe_3$), 3.69 (s, 6 H, OMe), 3.73 (s, 6 H, OMe), 6.61 (d, ^3J = 8.4 Hz, 2 H, [a/a′]-H), 6.65 (d, ^3J = 8.4 Hz, 2 H, [a/a′]-H), 7.29 (t, ^3J = 8.4 Hz, 1 H, b-H), 7.29 (t, ^3J = 8.4 Hz, 1 H, b′-H), 7.62 (d, ^3J = 8.0 Hz, 1 H, 8-H), 7.74 (d, ^3J = 8.8 Hz, 1 H, 6-H), 7.80 (d, ^3J = 8.8 Hz, 1 H, 5-H), 8.21 (d, ^3J = 8.0 Hz, 1 H, 7 H), 8.35 (s, 1 H, 4-H); ^{13}C NMR (100 MHz, $CDCl_3$) δ −0.3, 56.1, 56.4, 99.0, 102.7, 104.5, 105.1, 119.3, 120.6 (2C), 125.7, 126.2 126.9 (2C), 128.0, 129.7 (2C), 135.3, 138.6, 145.0, 146.0, 155.2, 157.4, 158.5 (2C); IR (KBr) ν 3417, 3001, 2957, 2939, 2898, 2836, 2152, 1643, 1616, 1599, 1590, 1538, 1505, 1473, 1458, 1432, 1412, 1397, 1359, 1305, 1286, 1250, 1214, 1185, 1173, 1112, 1068, 1036, 1023, 997, 912, 891, 859, 843, 781, 761, 732, 643; ESI-MS m/z (%) 549.3 (100) $[M + H]^+$. Anal. Calcd for $C_{33}H_{32}N_2O_4Si \cdot H_2O$: C, 69.94; H, 6.05; N, 4.94. Found: C, 70.35; H, 5.75; N, 4.93.

2,9-Bis(2,6-dimethoxyphenyl)-3-ethynyl[1,10]phenanthroline (11). Yield 97%; mp > 260 °C; ^{1}H NMR (400 MHz, $CDCl_3$) δ 3.05 (s, 1 H, ethynyl), 3.71 (s, 6 H, OMe), 3.73 (s, 6 H, OMe), 6.63 (d, ^3J = 8.4 Hz, 2 H, [a/a′]-H), 6.66 (d, ^3J = 8.4 Hz, 2 H, [a/a′]-H), 7.30 (t, ^3J = 8.4 Hz, 1 H, [b/b′]-H), 7.31 (t, ^3J = 8.4 Hz, 1 H, [b/b′]-H), 7.64 (d, ^3J = 8.0 Hz, 1 H, 8-H), 7.76 (d, ^3J = 8.8 Hz, 1 H, 6-H), 7.82 (d, ^3J = 8.8 Hz, 1 H, 5-H), 8.22 (d, ^3J = 8.0 Hz, 1 H, 7 H), 8.42 (s, 1 H, 4-H); ^{13}C NMR (100 MHz, $CDCl_3$) δ 56.2, 56.4, 80.9, 81.3, 104.6, 105.1, 118.9, 119.7, 120.4, 125.6, 126.4, 126.9, 127.0, 128.0, 129.8, 129.9, 135.4, 139.9, 145.3, 146.0, 155.3, 156.8, 158.5 (2C); IR (KBr) ν 3414, 3285, 3002, 2939, 2904, 2836, 1641, 1620, 1598, 1590, 1539, 1505, 1473, 1458, 1431, 1413, 1398, 1358, 1304, 1286, 1251, 1215, 1173, 1109, 1065, 1033, 1022, 988, 918, 892, 842, 781, 766, 731, 652; ESI-MS m/z (%) 477.2 (100) $[M + H]^+$. Anal. Calcd for $C_{30}H_{24}N_2O_4 \cdot H_2O$: C, 72.86; H, 5.30; N, 5.66. Found: C, 72.68; H, 5.16; N, 5.42.

Synthesis of 6. 2,9-Bis(2,6-dimethoxyphenyl)-3-ethynyl[1,10]-phenanthroline (**11**; 200 mg, 420 μmol), 1,4-bis(decyloxy)-2,5-diiodobenzene (135 mg, 210 μmol), TBAF·$3H_2O$ (800 mg, 2.54 mmol), and *trans*-$PdCl_2(PPh_3)_2$ (9.50 mg, 13.5 μmol) were combined in a Schlenk flask under nitrogen atmosphere. The solid mixture was stirred at 80 °C for 12 h. Then, it was cooled, dissolved with dichloromethane, and washed successively with aqueous KOH (100 mL) and water (5 × 200 mL). After drying over Na_2SO_4, the organic solvent was removed under reduced pressure. The crude product was purified using column chromatography (SiO_2; 19:1 CH_2Cl_2/EtOAc) affording **6** as yellow solid. Yield 66%; mp 247 °C; ^{1}H NMR (400 MHz, CD_2Cl_2) δ 0.88 (t, ^3J = 6.8 Hz, 6 H, CH_3), 1.30−1.51 (m, 24 H, CH_2), 1.54−1.59 (m, 4 H, CH_2), 1.79−1.86 (m, 4 H, CH_2), 3.71 (s, 12 H, OCH_3), 3.72 (s, 12 H, OCH_3), 3.87 (t, ^3J = 6.8 Hz, 4 H, OCH_2), 6.30 (s, 2 H, c-H), 6.71 (d, ^3J = 8.4 Hz, 4 H, [a/a′]-H), 6.73 (d, ^3J = 8.4 Hz, 4 H, [a/a′]-H), 7.38 (t, ^3J = 8.4 Hz, 2 H, [b/b′]-H), 7.41 (t, ^3J = 8.4 Hz, 2 H, [b/b′]-H), 7.58 (d, ^3J = 8.2 Hz, 2 H, 8−7.83 (d, ^3J = 8.8 Hz, 2 H, 6-H), 7.89 (d, ^3J = 8.8 Hz, 2 H, 5-H), 8.30 (d, ^3J = 8.2 Hz, 2 H, 7-H), 8.42 (s, 2 H, 4-H); ^{13}C NMR (100 MHz, CD_2Cl_2) δ 14.5,

(27) Gale, P. A. *Philos. Trans. R. Soc. London, A* **2000**, *358*, 431.

(28) Dumur, F.; Mayer, C. R.; Dumas, E.; Marrot, J.; Sécheresse, F. *Tetrahedron Lett.* **2007**, *48*, 4143.

23.3, 26.7, 29.8, 30.0, 30.1, 30.3, 30.4, 32.5, 56.5, 56.6, 70.2, 91.8, 93.0, 104.3, 104.4, 114.3, 117.9, 119.1, 120.0, 121.3, 126.3 (2C), 127.6, 127.7, 128.5, 130.3, 130.4, 136.3, 138.5, 145.5, 146.6, 153.5, 156.3, 157.5, 158.7, 159.0; IR (KBr) ν 3426, 3006, 2926, 2853, 2838, 1636, 1616, 1599, 1590, 1538, 1500, 1473, 1459, 1431, 1391, 1357, 1304, 1285, 1276, 1250, 1214, 1173, 1111, 1064, 1033, 1022, 996, 910, 891, 844, 781, 767, 732, 655; ESI-MS *m/z* (%) 1339.8 (100) $[M + H]^+$. Anal. Calcd for $C_{86}H_{90}N_4O_{10}\cdot 2H_2O$: C, 75.08; H, 6.89; N, 4.07. Found: C, 75.11; H, 6.71; N, 4.04.

Synthesis of 7. A procedure similar to that for the preparation of **6** was followed by reacting the corresponding precursors **12** (100 mg, 489 μmol) and **13** (213 mg, 489 μmol) with *trans*-$PdCl_2(PPh_3)_2$ (20.0 mg, 28.5 μmol) and TBAF$\cdot 3H_2O$ (925 mg, 2.93 mmol). Yield 83%; mp 242 °C; ^{1}H NMR (400 MHz, $CDCl_3$) δ 7.38 (ddd, ^3J = 7.6 Hz, ^3J = 4.8 Hz, ^4J = 1.2 Hz, 2 H, f″-H), 7.66 (d, ^3J = 8.2 Hz,^3J = 4.4 Hz, 1 H, 8″-H), 7.78 (d, ^3J = 8.4 Hz, 2 H, a″-H), 7.81 (d, ^3J = 8.8 Hz, 1 H, 6″-H), 7.85 (d, ^3J = 8.8 Hz, 1 H, 5″-H), 7.90 (dt, ^3J = 7.6 Hz, ^4J = 2.0 Hz, 2 H, e″-H), 7.97 (d, ^3J = 8.4 Hz, 2 H, b″-H), 8.27 (dd, ^3J = 8.2 Hz, ^4J = 1.8 Hz, 1 H, 7″-H), 8.44 (d, ^4J = 2.0 Hz, 1 H, 4″-H), 8.69 (d, ^3J = 7.6 Hz, 2 H, d″-H), 8.75 (ddd, ^3J = 4.8 Hz, ^4J = 2.0 Hz, ^5J = 1.0 Hz, 2 H, g″-H), 8.78 (s, 2 H, c″-H), 9.22 (dd, ^3J = 4.4 Hz, ^4J = 1.8 Hz, 1 H, 9″-H), 9.33 (d, ^4J = 2.0 Hz, 1 H, 2″-H); ^{13}C NMR (100 MHz, CD_2Cl_2) δ 88.4, 93.6, 119.0, 119.8, 121.7, 123.8 (2C), 124.5, 126.6 127.9, 128.0, 128.4, 129.7, 132.9, 136.5, 137.4, 138.6, 139.5, 145.5, 146.6, 149.6, 149.7, 151.0, 152.4, 156.5, 156.7; IR (KBr) ν 3408, 2360, 2207, 1654, 1604, 1585, 1566, 1542, 1514, 1502, 1467, 1443, 1421, 1388, 1264, 1099, 1076, 1039, 991, 906, 831, 788, 729, 687, 661; ESI-MS *m/z* (%) 512.3 (100) $[M + H]^+$. Anal. Calcd for $C_{35}H_{21}N_5\cdot CH_2Cl_2$: C, 72.49; H, 3.89; N, 11.74. Found: C, 72.52; H, 3.79; N, 11.46.

Self-Assembly of Trapezoid T. At ambient atmosphere, a mixture of **6** (5.20 mg, 3.88 μmol), **7** (3.97 mg, 7.76 μmol), and $Zn(OTf)_2$ (2.82 mg, 7.76 μmol) was refluxed in acetonitrile for 2 h until a clear yellow solution was obtained. After addition of solid $[Cu(MeCN)_4](PF_6)$ (2.89 mg, 7.76 μmol) and **5** (4.13 mg, 3.88 μmol) the solution was further refluxed for 8 h. The resulting orange-red solution was characterized without further purification. Yield quantitative; mp > 260 °C; ^{1}H NMR (400 MHz, CD_3CN) δ 0.78 (t, ^3J = 6.8 Hz, 6 H, CH_3), 1.17−1.20 (m, 28 H, CH_2), 1.37 (s, 3 H, CH_3) 1.37−1.40 (m, 4 H, CH_2), 1.45 (s, 3 H, CH_3), 1.48 (s, 3 H, CH_3), 1.50 (s, 3 H, CH_3), 1.58 (s, 3 H, CH_3), 1.62 (s, 3 H, CH_3), 1.67 (s, 3 H, CH_3), 1.69 (s, 6 H, CH_3), 1.71 (s, 3 H, CH_3), 1.73 (s, 3 H, CH_3), 1.76 (s, 3 H, CH_3), 1.78 (s, 3 H, CH_3), 1.82 (s, 3 H, CH_3), 2.71 (s, 3 H, OCH_3), 2.72 (s, 3 H, OCH_3), 2.73 (s, 6 H, OCH_3), 2.84 (s, 9 H, OCH_3), 2.85 (s, 3 H, OCH_3), 3.59 (t, ^3J = 6.4 Hz, 2 H, OCH_2), 3.61 (t, ^3J = 6.4 Hz, 2 H, OCH_2), 5.87−6.08 (m, 12 H, mesityl-, a-, a′-H), 6.37 (s, 1 H, c-H) 6.40 (s, 1 H, c-H) 6.73 (t, ^3J = 8.0 Hz, 1 H, [b/b′]-H), 6.75 (t, ^3J = 8.0 Hz, 1 H, [b/b′]-H), 6.87 (t, ^3J = 8.4 Hz, 2 H, [b/b′]-H), 7.46−7.50 (m, 4 H, f″-H), 7.62−7.66 (m, 4 H, g″-H), 7.76−7.88 (m, 4 H, 8″-, a″-H), 7.92 (d,^3J = 8.4 Hz, 2 H, a″-H), 7.96−8.08 (m, 8 H, 5″-, 6″-, 8-, 8′-H), 8.17−8.25 (m, 9 H, b″-, e″-,6′-H), 8.29 (d,^3J = 9.2 Hz, 1 H, 6′-H), 8.31 (d,^3J = 9.2 Hz, 1 H, 5′-H), 8.36 (d,^3J = 9.2 Hz, 1 H, 5′-H), 8.42 (d,^3J = 9.2 Hz, 2 H, 6-H), 8.49−8.51 (m, 10 H, 4″-, 5-, [2″/9″]-, d″-H), 8.61 (s, 2 H, c″-H), 8.64 (d,^3J = 7.2 Hz, 2 H, [2″/9″]-H), 8.68 (s, 2 H, c″-H), 8.72−8.75 (m, 2 H, 7″-H), 8.82 (d, ^3J = 8.4 Hz, 1 H, [7/7′]-H), 8.84 (d, ^3J = 8.4 Hz, 1 H, [7/7′]-H), 8.90 (s, 1 H, [4/4′]-H), 9.04 (d, ^3J = 8.4 Hz, 1 H, [7/7′]-H),), 9.04 (d, ^3J = 8.4 Hz, 1 H, [7/7′]-H), 9.06 (s, 1 H, [4/4′]-H), 9.07 (s, 1 H, [4/4′]-H), 9.11 (s, 1 H, [4/4′]-H); IR (KBr) ν 3475, 3072, 2924, 2853, 2361, 2341, 2211, 1617, 1602, 1590, 1575, 1549, 1500, 1476, 1428, 1403, 1363, 1278, 1256, 1224, 1160, 1111, 1070, 1031, 1018, 914, 843, 791, 747, 736, 725, 694, 668, 659, 638; ESI-MS *m/z* (%) 614.4 (100), $[M - 2PF_6, 4OTf]^{6+}$, 766.5 (90), $[M - 2PF_6, 3OTf]^{5+}$, 995.6 (18), $[M - 2PF_6, 2OTf]^{4+}$, 1376.9 (8) $[M - 2PF_6, OTf]^{3+}$. Anal. Calcd for $C_{226}H_{188}Br_2Cu_2F_{24}N_{18}O_{22}P_2S_4Zn_2\cdot 2H_2O$: C, 58.91; H, 4.20; N, 5.47; S, 2.78. Found: C, 58.45; H, 3.69; N, 5.28; S, 2.51.

Acknowledgment. We are thankful to the Deutsche Forschungsgemeinschaft and the University of Siegen for financial support of this research. Support from the DAAD for K.M. (Promotionsabschlussstipendium) is gratefully acknowledged.

Supporting Information Available: ^{1}H NMR, ^{13}C NMR, and ESI spectra of all relevant compounds and details of the DPV investigations and the deconvolution. This material is available free of charge via the Internet at http://pubs.acs.org.

JA907185K